International Journal of Advanced Multidisciplinary Research and Educational Development
Volume 2, Issue 2 | March – April 2026 | www.ijamred.com
ISSN: **3107-6513**

Reduction of Losses in Energy Distribution by Reconfiguration of The Network Using New Optimization Technique

Muhammad Khurshid Ahmad[1], Muhammad Aslam[1], Abdullah Khan[*]

[1] *US-Pakistan Center for Advanced Studies in Energy University of Engineering and Technology, Peshawar*

[*]*corresponding.author:* *engr.abdullahkhan23@gmail.com*

Abstract

This research investigates the optimization of electrical power distribution networks with the primary objective of minimizing active power losses and enhancing voltage profiles through intelligent network reconfiguration. The study focuses on the IEEE 33-bus and 69-bus radial distribution systems and employs the Grey Wolf Optimization (GWO) algorithm—a meta-heuristic inspired by the cooperative hunting behavior of grey wolves—to determine optimal switching configurations of sectionalized and tie switches while maintaining network reliability and radial topology constraints. The proposed GWO-based reconfiguration model incorporates multi-objective functions that simultaneously address active and reactive power loss reduction indices and voltage profile improvement indices. Power flow analyses are conducted using the Newton-Raphson method to validate system performance before and after reconfiguration. Simulation results reveal significant improvements: for the IEEE 33-bus system, active power loss is reduced by 23.83% and reactive power loss by 3.90%, while voltage magnitude improved from 0.9107 pu to 0.9212 pu. Similarly, for the IEEE 69-bus system, active and reactive power losses decreased by 46.99% and 5.35%, respectively, with the minimum voltage rising from 0.9091 pu to 0.9482 pu. The findings demonstrate that the GWO algorithm outperforms traditional optimization techniques in achieving rapid convergence, superior power loss minimization, and enhanced voltage stability. The study establishes GWO as a robust and computationally efficient tool for real-time distribution network reconfiguration, contributing to improved operational efficiency and loss mitigation within modern smart grid systems.

Keywords: *Power Distribution Network, Network Reconfiguration, Grey Wolf Optimization, Meta-Heuristic Algorithms, Power Flow Analysis, Active Power Loss Reduction, Reactive Power Loss Reduction, Smart Grid Optimization*

Introduction

Power Systems are basically networks consisting of three systems including transmission system, distribution system and generation system. Generation system is used to generate electrical energy by using different sources and methods such as Hydro, Thermal, Renewable energies (Solar, Tidal, Geothermal, Wind etc). Transmission system is used to Transmit that energy to Grids for where distribution system distributes the energy to consumers according to demand [1]. Each of these three systems have their own efficiency parameters, we will work on distribution system. Minimization of active powers loss and improving the voltages profile many methods can be used but we will focus on the most suitable network reconfigurations of distribution system networks by altering ties and sectionalize switch by keeping the reliability of the networks intact. To find the best switching pattern which leads to minimized active power losses in distribution system different type of optimization algorithm can be used like Artificial Bees colony (ABC), Fireworks Algorithm (FWA), Artificial Neural Networks (ANN), but we will use Grey Wolf Optimization (GWO).

Literature Review

Various optimization techniques have been developed for Distribution Network Reconfiguration (DNR) to improve the voltage profile and reduce active power losses in distribution systems. Early approaches used the Branch and Bound method, where the network is initially converted into a meshed structure and switches are sequentially opened to achieve a radial configuration,

ISSN: 3107-6513

although this method required high computational time. Later improvements introduced sequential switching strategies to enhance efficiency.

In recent years, several metaheuristic algorithms have been applied to the DNR problem, including the Fireworks Algorithm, Bacterial Foraging Optimization Algorithm, Genetic Algorithm, Ant Colony Optimization, Cuckoo Search Algorithm, Artificial Immune Algorithm, and Particle Swarm Optimization. These techniques aim to determine the optimal network configuration that minimizes power losses and improves system performance. Other approaches such as Simulated Annealing, convex optimal power flow methods, fuzzy-based optimization, and capacitor placement techniques have also been explored to further enhance distribution network efficiency. A comparison of these optimization techniques is typically presented to evaluate their effectiveness in loss reduction and voltage profile improvement.

Research Motivation

The most fragile link in Pakistan is the distribution system within the entire power sector. This system contains around 17% of the transmission loss whereas the distribution loss is about 20% of entire power systems distribution networks. The major portion of total power loss happens in the distribution lines. Its key reasons include longer distribution cable, technical loss, lower power factors of primary and secondary distribution networks and lower voltages within distribution networks. In order to remain competitive, it is essential for power distribution firms to fulfil the demands of their consumers effectively. This means that one of their goals is finding an operating state for a large, balanced, three-phase distribution network. The increase in population becomes the major cause of increase in demand for electricity.

Problem Statement

Today's distribution systems have attained complexity. The enhancement in the present draw due to the distribution of electric current has resulted in the instability which frequently causes power loss. This problem can be solved by coordinated reconfiguration and upgrading of the distribution system in the changing load conditions.

Research Methodology

The methodology of this research involves several key steps. Initially, data for the IEEE 33-bus radial distribution network is collected. A suitable method is then established to perform power flow analysis for the distribution system in order to estimate the initial configuration of the network. After that, a Grey Wolf Optimization (GWO) algorithm is developed to determine the optimal sectionalizing switches while considering active power losses and voltage profile improvement. Finally, the developed model is tested and validated, and the reconfigured network is compared with the original system to evaluate the reduction in power losses and overall performance improvement.

Aims and Objectives

The main objective of this study is to minimize system losses and enhance voltage profiles through optimal distribution network reconfiguration. This is achieved by formulating multi-objective functions that consider the Active Power Loss Reduction Index (PLRI), Reactive Power Loss Reduction Index (QLRI), and Voltage Profile Improvement Index (VPII). Additionally, voltage profiles are analyzed both before and after network reconfiguration to determine the optimal network configuration that provides improved system performance.

Contribution to Knowledge

The current research study will enable engineers to monitor and analyse distribution network on real time basis. As the research is aimed at applications of electrical engineering, so the project will have an effective scope in distribution industries as well. As such work has not been done in Pakistan so the research will open a new dimension of study and its application will also contribute in improving the line losses in Pakistan. Sensitive loads which are at load bus are more secured from voltage sag/swell problems. This also results in reduction distribution network losses and results in optimum power flow in the distribution network.

ISSN: 3107-6513

1. Methodology

1.1 The Power System design

This section describes the basic structure and components of electric power systems, including generation, transmission, and distribution subsystems. Power systems consist of multiple interconnected networks that generate electrical energy from sources such as hydro, thermal, wind, and nuclear plants, which is then transmitted at high voltage levels using transformers to reduce losses over long distances. The power is subsequently delivered through sub-transmission and distribution networks to industrial, commercial, and residential consumers at appropriate voltage levels. Most power systems operate using three-phase alternating current (AC) and include major equipment such as generators, transformers, and motors, enabling reliable electricity supply across large geographical areas.

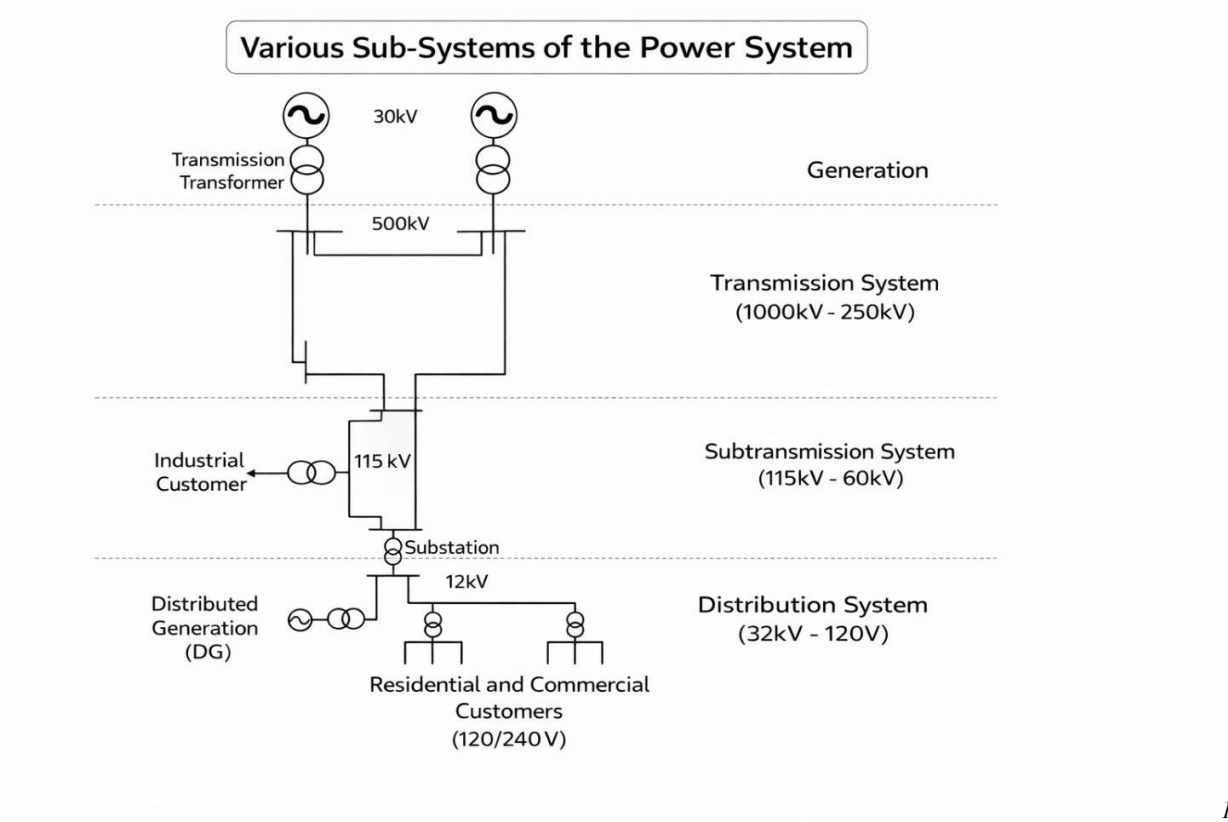

Figure 1. various sub-systems of the Power system

1.2 Electric Power Distribution System

It is the final stage of the whole system. These distribution mechanisms operate through voltage step downing and the protection devices called the 'substation.' In this substation, higher voltage transmission line is decreased by the transformer for supplying to the consumers gathered at distribution layers. It is important for understanding the arrangements and constituents of distribution system to analyze the functions of elements making up power distribution systems. The power flow study essentially needs the already known topology of distribution systems by manipulating the constituents including switch and power line.

1.3 Radial Distribution Networks

Power distribution systems are traditionally designed using a radial network topology. For analytical studies, the distribution network can be modeled as a graph structure, specifically a tree graph, where buses are represented as nodes and power lines as edges (branches). A tree graph is a connected network without closed loops, meaning that no branch splits and reconnects to form a cycle. In graph theory, a network with n nodes forms a tree if it is connected and contains exactly (n−1) edges. In this

ISSN: 3107-6513

study, each line segment is assumed to be equipped with a switching device, therefore the number of edges is equal to the number of switches, with each switch controlling a single line segment.

$$Nedg = n - 1 \quad \text{.....Eq (1)}$$

1.4 Distribution Network

Distribution networks are often characterized by their radial structure, meant to carry electric power from the substation to all the existing loads interconnected to the network. Below Figure shows represents a singular line drawing of a 16-bus radial distribution networks. The feeder bus must enable to endure the summation of load demand at the subsequent nodes and the power loss within the line segment. In strict terms, the loading of the feeder bus can be described as follows:

$$F = \sum Nn = 1 P_n + P_{loss} \quad \text{..... Eq (2)}$$

Here PF is the feeding power given to networks by the feeder bus, N stands for the number of nodes, $Ploss$ refers to load power demand at bus n and $Ploss$ are the power loss within the lines. During distribution systems analysis, it is common practice to consider the feeder bus as the source node, and loads, generator or other components are expected to be interconnected at the subsequent nodes.
Figure 2 represents the radial network diagram of a power system.

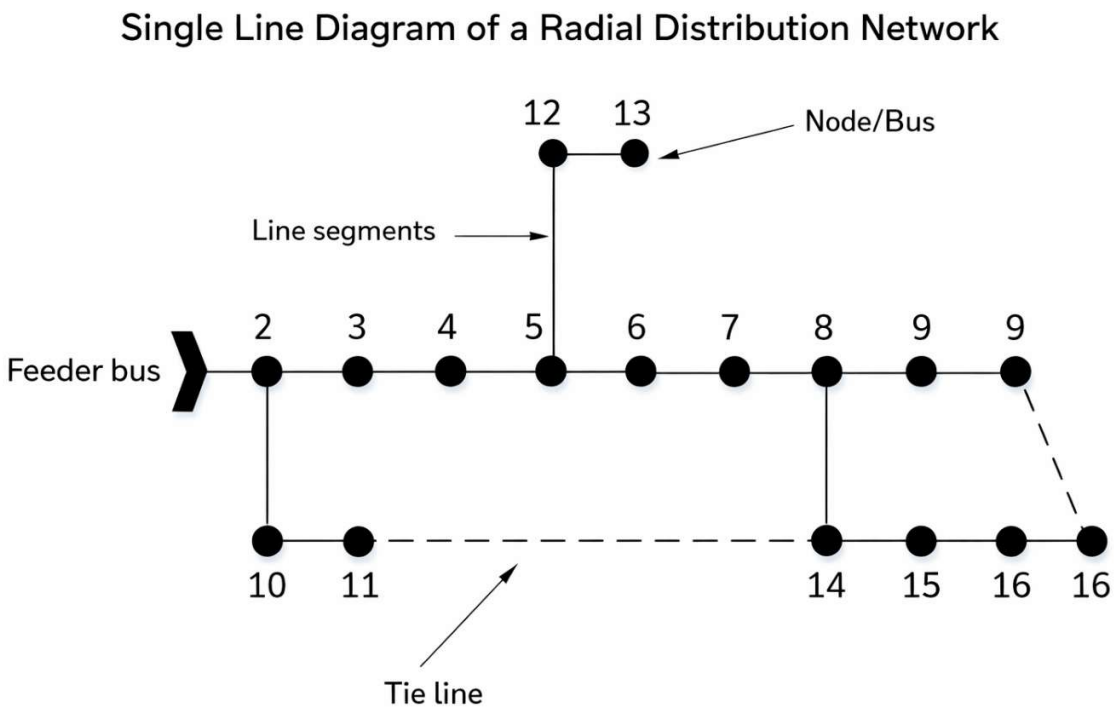

Figure 2. Single line diagram or a radial distribution network

1.5 Voltage Drop Calculation

Voltage drop analysis is a critical aspect of distribution system design and reconfiguration studies, where minimizing voltage deviations along feeder lines is often an objective. Voltage drop influences line losses and the performance of distribution components under constant PQ load conditions. Referring to Figure 3, which depicts a single-line diagram of a power line segment, if the sending-end voltage at node *i*, Vi∗V_i^*Vi∗, is known, the receiving-end voltage at node *i+1*, Vi+1∗V_{i+1}^*Vi+1∗, can be calculated as:

V⃗i+1=V⃗i−I⃗i,i+1(Ri+jXi)(Eq. 3)\vec{V}_{i+1} = \vec{V}_i - \vec{I}_{i,i+1} (R_i + jX_i) \quad \text{(Eq. 3)}Vi+1=Vi−Ii,i+1(Ri+jXi)(Eq. 3)

ISSN: 3107-6513

Subsequently, the voltage drop across the line segment is obtained by:
ΔV=V⃗i−V⃗i+1(Eq. 4)\Delta V = \vec{V}_i - \vec{V}_{i+1} \quad \text{(Eq. 4)}ΔV=Vi−Vi+1(Eq. 4)
This formulation links the line impedance and current flow directly to voltage deviations along the feeder.

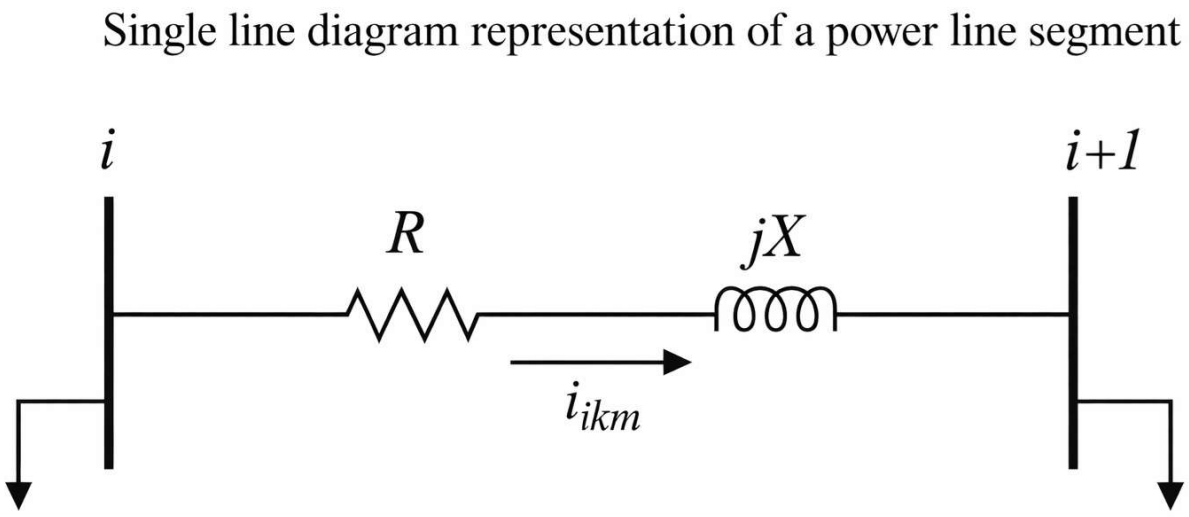

Figure 3. Single line diagram representation of a power line segment

1.6 Power Loss Calculation

Most of the power losses present in power systems are due to resistive losses (I 2R) given in the power lines, although losses given in other equipment (e.g. transformers) can be considerable [4]. The power loss within distribution system is around 70% of the entire power loss [5], consequently, utility companies often search for solutions to minimize operational costs related to electric power delivery and power losses are no exception. Recent developments of Smart grid technology and distributed generation represent an incentive for power engineers to develop methodologies applied to the reduction of power losses which directly minimize operational.

1.7 Line Impedance Calculation

Line impedance is a critical parameter to be determined for it is necessary when modelling power systems. Impedance is phenomena present in AC circuits and it is the measure of opposition that a circuit presents to a current when voltage is applied. One particular parameter when working with power lines is series impedance which consists of conductor resistance and self and mutual inductive reactance as a result of magnetic fields around conductors [6]. Conductor manufacturers typically provide conductor resistance; however, reactance is to be determined for it is case specific. Figure 4 shown below, shows conductors 1 to N with respective magnetic fluxes created by current flow in the conductor. Based on the assumption that current flows out the page the sum of all the currents in all lines is equal to zero as expressed by

$$I1 + I2 + \ldots + IK + \ldots + In = 0 \quad \ldots\ldots \qquad \text{Eq (5)}$$

The total flux linking conductor is:

$$\lambda_k = N.\phi = 2.10^{-7}.\left(I_1.\ln\left(\frac{1}{D_{K1}}\right) + I_2.\ln\left(\frac{1}{D_{K2}}\right) + \cdots + I_k.\ln\left(\frac{1}{GMRD_K}\right) + \cdots + I_n.\ln\left(\frac{1}{D_{Kn}}\right)\right)$$

…..Eq (6)

Here N shows the amount of times flux surrounds the conductor Dkn refers to the separation between the two conductors i and k. GMRk denotes geometric mean radius for the conductor k. Conductor inductance composes of self-inductance and mutual inductance of conductor k and the rest k-1 conductors. Self-inductance and mutual inductance units are henry per meter [H/m] and express by equations 7 and 8 respectively.

$$L_{kk} = \frac{\lambda_{kk}}{I_k} = 2.10 - 7.\ln\left(\frac{1}{GMR_K}\right)[H/m] \qquad \text{Eq (7)}$$

$$L_{kn} = \frac{\lambda_{kn}}{I_n} = 2.10 - 7.\ln\left(\frac{1}{D_{kn}}\right)[H/m] \qquad \text{Eq (8)}$$

ISSN: 3107-6513

where: Dkn is the distance between conductor k and conductor n. Assuming a three phase balanced system and power lines transposed, self and mutual inductance can be determined [7] as follows:

$$L_k = \frac{\lambda_{kn}}{I_n} = 2.10 - 7.\ln\left(\frac{\mathrm{D_{eq}}}{\mathrm{GMR_k}}\right)[\mathrm{H/m}] \quad \text{Eq (9)}$$

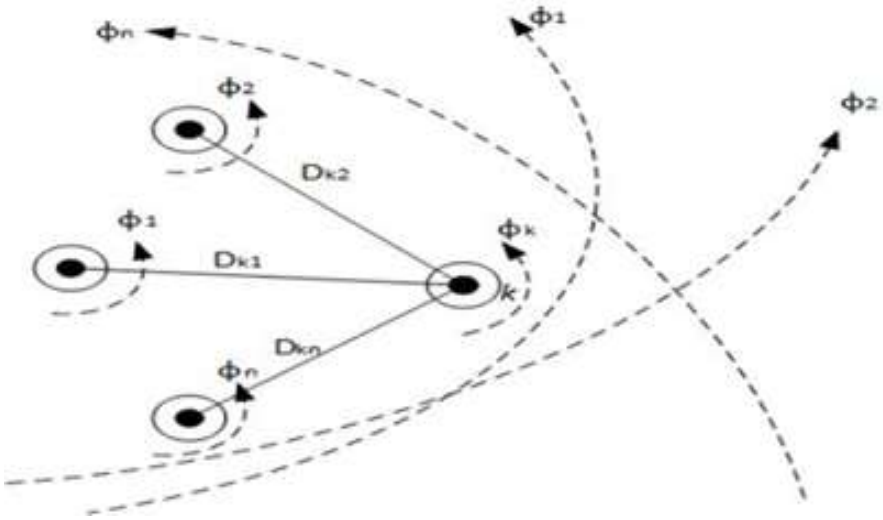

Figure 4. Magnetic fields present in conductor lines

Where: Dre is the equivalent distances between phases a,b, and expressed as :

$$D_{eq} = \sqrt{D_{ab} - D_{bc} - D_{cn}} \quad \text{Eq (10)}$$

Given operational frequency, the inductive reactance is given as:

$$X_i = \omega.\ln\left(\frac{D_{eq}}{GMR_k}\right)[\Omega/(m, km, mile)] \quad \text{Eq (11)}$$

Typically, power distribution systems operate with un-transposed power lines and unbalanced phases], therefore other methods considering these factors in addition to ground and neutral line influences have been developed such as Carson's equations. Carson's equations were not used due to the high number of calculations involved which was considered tedious until the introduction of digital computers. Computers have allowed for the wide use of Carson's equations and modified equations.

1.8 Power Flow Analysis

The analysis of a power distribution network under steady state operation lays essentially on a power flow simulation. Power flow simulations in distribution systems may intuitively be though similar to those of transmission networks and that is true at a certain extent, however, their network topology differ significantly. In radial distribution systems, methods used in transmission systems are not applied "because of poor convergence characteristics". In meshed and weakly meshed distribution networks, other techniques may be applied. Section two and three present detailed information on power flow methods applied to power distribution systems. Power flow analysis often determines the following parameters [8].

- Apparent, real, and reactive power flows
- Instant voltage magnitudes and per unit values at the buses of the network
- Power Losses given across lines, transformers, capacitors, etc.
- Voltage and current angle deviations

1.9 Power Distribution Network Reconfiguration

DNR attempts to change configuration of a distribution networks through changing the position of existing tie and sectionalized switch

ISSN: **3107-6513**

to minimize or maximize certain operational characteristics such as power losses. Minimum bus voltage level maximization is often one of the objective functions of major importance when DNR is implemented [9].

$$\max\ (minV_i) \qquad \text{Eq (12)}$$

Some of constraints when applying DNR are:

Bus voltage Constraint. Here, operational voltage standards should always be met when reconfiguring the system, in strict terms, voltage values at all buses of the system should not be lower than the minimum voltage Vmin of greater than the maximum voltage value Vmax:

$$V_{mini} < V_i < V_{maxi} \qquad \text{Eq (13)}$$

2. After reconfiguration, all power lines must be operating within their thermal limits:

$$I_i < I_{maxi} \qquad \text{Eq (14)}$$

Where Ii is the current carried by line segment i and Iimax is the maximum ampacity of the line segment i.

3-Typically, power distribution networks adopt a radial topology. When performing DNR, the network topology of the distribution system must be kept at all times to be considered a feasible solution:

$$g_i \ \epsilon \ G_{radial} \qquad \text{Eq (15)}$$

Where gi is the network configuration obtained after DNR and $Gradial$ represents a set of all possible radial configurations corresponding to a given system.

4. When working with large distribution networks, some exhaustive methods might be prohibitive due to computational power limits. DNR not only requires the computation of complex DNR algorithms, but to compute power flow analysis, which can be considerable

1.10 Feeder Reconfigurations

Reconfigurations of distribution networks (RODN) constitute the most essential role of distribution system operations. Its main aim is selecting the on/off position of the sectionalized switch for the optimizations of distribution systems (given in Fig.5) for reducing the voltages deviation along with balancing the load and reducing the line loss [10].

Figure 5. Basic concept of Reconfiguration of distribution network (RODN).

Load balancing through feeder configuration is necessary to utilize in which various feeders form the feeding area along with the congested loads. For balancing the load of the network, the operators arrange supplied paths of the load to other portions of the networks. This is decided by feeder load management where they detect crucial positions and indicates to regulate the entire distribution systems by identifying hazardous places to warn the distribution operator for paying attention to the areas where needed. Requiring more fast decision, the computation supports and correct the current issue in order to enhance sustainability and energy deliverance performance of distributive network. Similarly, loss reduction becomes the other targets of feeder reconfigurations. In this process, the entire revenue and energy loss

ISSN: 3107-6513

need to be reduced for efficient operations for operating the utility networks in the maximized ability or operations constraint without predicting the results of fault occurring. DMS applications use switch management applications for optimizing the networks. Meanwhile, the loss reduction issue is resolved through optimal power flow functions resulting in the realization of optimal operation. In mathematics, the issue of RODN is considered as a combinatorial nonlinear optimizations issue that is not easy to resolve in an applied computational time. The comprehensive mathematical definition of RODN is discussed in every chapter on the basis of various situations.

1.11 Meta-heuristic Reconfiguration Method

Various algorithms are developed for RODN. In the previous researches, the key approach deals with the application of meta-heuristic algorithm. Various algorithms for RODN are produced. In the earlier development, the key approach includes the applications of meta-heuristic algorithm. The ant colony search (ACS) methodology aimed to research for the optimum path within graphs on the basis of behaviors of ants trying to seek a location between their colonies and their food sources. ACS was used to resolve configuration issue in [11]. Within the ACS, the application of the optimistic feedback methodology requires quick search and the distributive computations to hire the ant colonies in order to avoid premature convergences. Within these particles given in the particle swarm optimization (PSO) shares the great knowledge of earlier most suitable solutions of particles and the most feasible solutions of the populations as well for leading the move towards their targeted places. This PSO begins with a population of randomized solution to search for optima through updated generation. Within PSO, the potential solution known as the particle flies via the problem spaces using current optimal particle. In EP methodology is used having the benefit of ensuring the radial topology of researched string. The grey correlation analysis (GCA) is utilized to resolve multi-objective issue within reconfiguration issue. In [12], Simulated annealing (SA) is essentially feasible for a great combinatorial optimization issue as it avoids local minima by showing enhancements in costs. On the other hand, it frequently needs a useful cooling schedule along with a particular strategy making usage of the attribute of distribution system for seeking the optimum solutions. The genetic algorithm (GA) process can attain global optimal solutions rather than other meta-heuristic research method while taking lesser time than the exhaustive research. This GA carries the benefit of utilizing presentation of objects called strings than utilizing the objects themselves; however, its major issue involves the coding of the object into a string. Everyday principles in meta-heuristic method are iterative circulation procedure that finds the optimum or sub-optimum solution within a modest algorithm but it needs longer computational time.

1.12 Heuristic Reconfiguration Method

As compared to the meta-heuristic or artificial intelligence skills, heuristic algorithm is more feasible to operate online. Optimal switch state including closed/opened switch is achieved one by one in heuristic approach; therefore, global optimality is not guaranteed. Despite this disadvantage, this approach provides a great benefit in computation stability by devising heuristics rule for avoiding unsuitable solution without using any heavier computation procedure. Branch exchange includes a classic heuristic methodology for RODN, and earlier researches [13] highlight that it is easier to be implemented and is feasible for online managements. The multiple tie (generally open) switch exists in the distribution systems. It can be exchanged to normal closed switch. The major disadvantage of branch exchange method lies in the definition of its earliest structure because the final results are dependent upon the earliest configuration so the burden of excess computational complexity is unavoidable and its results will be not certain. A hybrid heuristic methodology comprising of a circular minimal branch current updated mechanism and a circular neighbor's chain updated technique defining the earliest configuration by turning on switches with minimized current via a singular loop iteratively is used and this method enables to improve the calculation accuracy manifold. In the total distribution systems have been decomposed into subsystems on the basis of the connectivity of area where an individual agent is allocated for every decomposed subsystem. A double stage process on the basis of branch exchange methodology is used to coordinate the reconfiguration of decomposed subsystem. Optimal configuration of the whole system is obtained by the collaboration of individual

ISSN: 3107-6513

agent where this decentralized approach greatly decreases the computational time. A heuristic computational methodology on the basis of firefly movement equation is put forward in aiming to minimize the wastes of line loss. The key goal of this research study involves the simulation of fire fly movements toward its prey or partner for matching the insect position where the insect location is discretized within the spaces corresponding to the locations of the switch in the electric systems. [14] represents an effective two staged methodology because the effectiveness of the process is enhanced after stemming from the usage of real powers losses sensitivity regarding impedance of the candidate branch. This process utilizes loss sensitivity within the initial stage where a branch exchange method in the later stage is utilized for refining the solutions, puts forward a reconfiguration algorithm devised for larger scale system. The heuristic algorithm begins as the system within a meshed position having the maneuverable switch to be closed. These switches are turned on step by step as per the order pre-decided on the basis of calculation of the minimized total systems loss utilizing load flow programs. The refinement of this process on the basis of branch status exchange is also discussed in this research study. The heuristic algorithm in begins as the maneuverable switch is opened and later it is closed leading to the minimized upsurge within the objective functions at every step. This objective function is described as the augmented loss divided by amplified load service. A simple loss formula is utilized as a rough index for the switch of the candidate; however, a complete 16 load flow calculations after every switch turning off is used to regulate accurate loss and constraints. The back track option reduces the algorithm's greedy research. The algorithm utilizes more computation time as compared to other processes; however, it regulates constraint and control action feasibly.

1.13 Reconfiguration Schedules

Despite the highly developed computation accuracy and velocity, the previous algorithm [15], known as short-term configuration method is not practical in system managements as their solution is attained by depending upon a singular time interval load data, but the load condition in distribution systems differs from one moment to another, particularly, the growth of DG's installation including photovoltaic (PV) generator, enlarging the difference in load condition in sizes and speeds. Based on this point of view, these results of short-term reconfiguration method very early on lose efficiency along with time-varying loads. The earlier work reconsidered the time- varying issue of load within network reconfiguration issue by the two common practices. The traditional norm is that reconfiguration is used to obtain a stable configuration at a specified amount of time like the initial time or the time of peak loads by neglecting the time-varying issue load. The other practice regards time-varying load by checking systems states giving optimal configurations for the entire time period; for instance, for more than a day. It is known as online reconfiguration and is valid when it is assumed that network comprises of remote operating tie switch. The benefit of this first practice is that a number of switchable operations is reduced. On the contrary, its drawback is that because of the unknown load nature, the fixed networking configuration is not constantly optimal for a time period particularly when the network is installed by a certain intermittent DG. The online reconfiguration may produce good decrease in voltage deviation as compared to secure configurations, the total cost of switch operation for online reconfigurations results in great revenues from decreased voltages deviation. Within this case, networking reconfigurations become inefficient due to economic reasons. Although used GA for seeking optimal combinations of reconfigurations examples, the configurations got via temporary reconfigurations method are still static for operating on time-varying loads for a longer time period between two reconfigurations examples.

2. CLASSICAL OPTIMIZATION TECHNIQUES

Ideal establishment and estimating of Distributed Generation (DG) in dispersed frameworks is consistently difficult undertaking for shoppers as well as utilities in regards to normal advantages considering the environmental, affordable and pragmatic perspectives. There are unmistakable strategies which can be used as a piece of contour the territory and magnitude of Distributed Generation(s) in a distributed control system to ensure reduced structure control deprivation and upgraded voltage characteristics. By considering this fact, thinking about the best enhancement systems with the objective that strong results are gotten, is needed. This is in light of the fact that, as communicated evil arrangements can't impact Genetic Algorithm's end arrangement conversely, hence are discarded as repetitions move on. In the research field in regards to DG estimating and situation different strategies are utilized to locate the ideal arrangement these incorporates Lambda Iteration Method, Linear Programming, Lagrange Multiplier Method, Newton-Raphson Method, Strawberry Plant Propagation Algorithm, and Particle Swarm Optimization Method. All of these have their very own preferences and impediments and reasonableness for various activities.

ISSN: 3107-6513

2.1 Newton-Raphson Technique

It is a procedure shaped to streamlining arrangements. It requires just a starting worth that can be taken under consideration as the underlying theory for discovering the arrangement for example a successive better guess for the genuine esteemed capacities.

$$x: f(x) = 0 \qquad \text{Eq(16)}$$

A single variable value is used in Newton-Raphson method for computing the best postulate by repeating the formula:

$$x_{n+1} = x_n - \frac{f(x_n)}{f(x_n)} \qquad \text{Eq(17)}$$

Newton-Raphson strategy is useful while processing the real power stream arrangement. It is widely demonstrated method to settle problems of mathematical statements identified with vitality gushing by utilizing the cycles. As of late it has hold a standardized placement in computing resolutions of power stream matters.

2.2 Particle Swarm Optimization (PSO)

This technique was first proposed by Kennedy and Eberhart [16]. It is inspired by the social behavior of different animals including insects, herds, birds and fishes. The basic strategy of this algorithm focuses on the collaborative search of different birds for finding food. In this algorithm, every member in the population is modelled as a particle. The possible solutions of the optimization problems are represented by the each. These sets are also known as swarm.

Position of particles in the search space is represented as $X_i = [x_{i1}, x_{i2}, x_{i3}, \dots\dots\dots\dots\dots x_{id}]$ The best position of the ith particle is recorded and represented by $Pbest_i = Pb_{i1}, Pb_{i2}, \dots.. Pb_{id}$.The ideal position of whole particles is denoted as: $Gbesti = Gb1, Gb2, \dots.. Gbd$.

The optimal position of the swarm is that of all the individual's optimal positions. The velocity and the positions updated by the following equations:

$$v_{id}^{k+1} = wv_{id}^{k} + c_1 r_1 \left(Pb_{id}^{k} - x_{id}^{k}\right) + c_2 r_2 \left(Gb_{d}^{k} - x_{id}^{k}\right) \qquad \text{Eq (18)}$$

$$x_{id}^{k+1} = x_{id}^{k} + v_{id}^{k+1} \qquad \text{Eq(19)}$$

In Eq 18 w is the inertia weight while c defines the learning factors. c1 finds the impact of best individual ($Pbid$) while c2 determines the best global (Gbd)), where c1

+ c2 ≤ 4; r1 and r2 are numbers in range of 0 up to unity. The inertial weight function w is computed using Eq 20:

$$w = w_{max} - \frac{w_{max} - w_{min}}{iter_{max}} x\ iter \qquad \text{Eq (20)}$$

the initial and final weight value is represented by $wmax$ and $wmin$ respectively;

2.3 Artificial Bee Colony (ABC) Algorithm

Basic idea behind artificial bee colony (ABC) algorithm was the intelligent behavior of the bees for finding food. It has been developed by Karaboga [17]. The bees shows a very intelligent behavior in selecting the location of the nest, hunting for the food as well as the navigation [18]. Bee effectively selects the labor for food hunting/foraging by using the self-organization. There is a classification of bees according to their tasks: employed bees, onlooker bees and scout bees. The task of employed bees is to find the food sources and hires the other bees for dancing. The decision of the food source is done according to the dance of the employed bees at the specific food source. This is done by the onlooker bees which stay in the hive. To find new unexplored sources is the duty of the scout bees. Whenever the new source is found, the employed bee move to the other source and these employed bees becomes the scout bees. The undiscovered sources are searched by the scout bees and enhance availability of food. Upon finding the food, employed bees do the waggle dance to inform others. This is the biggest source of communication between the bees. The shared information includes the food quantity and position of the source. Artificial Bee algorithm uses a population of food source positions. Comparing with the optimization problem, every food source provides an alternative solution to the optimization problem while the amount of nectar is considered as the fitness of the solution. The optimum solution of the optimization problem refers to the most profitable source in the bee colony, it could be easily evaluated by considering the local and global search mechanisms.

In the first step food source population is generated randomly according to the Eq21

$$x_{ij} = x_j^{min} + rand(0,1)\left(x_j^{max} - x_j^{min}\right) \qquad \text{Eq (21)}$$

ISSN: 3107-6513

The range of i = 1 ... SN, and SN refers to the quantity/number of available food sources, whereas j = 1 ... D, and D defines the number of design parameters, while the upper bound of the j dimension is x_j^{max} and the lower bound is x_j^{min} .

In the employed Bee Phase, the neighbor food source is determined by using the Eq22

$$v_{mj} = x_{mj} + \varphi_{mj}(x_{mj} - x_{kj}) \quad \text{Eq (22)}$$

whereφmi is a random number with the range of [-1,1]. A local search is done according to the Eq 27 for finding the optimal solution (food) only the j parameter referring to the current location changes. After that, there is a comparison of the available food and selection of the better one. It is employed on every available food/solution and the better solution retains in the population.

In the onlooker bee phase, like the employed phase there is search of better solution. But the search is not conducted stochastically according to the fitness solution rather than searching each available solution/food source which leads to the selection of high-quality solutions. A probability (Eq 23) is assigned to each solution which is proportional to its fitness value.

$$p_i = \frac{fitness_i}{\sum_{i=}^{SN} fitness_{i_i}} \quad \text{…..Eq (23)}$$

2.4 Mine Blast Algorithm (MBA)

Mine blast algorithm is an optimization tool based on the idea of mine bomb explosion, proposed by the Sadollah et al [19]. During the process, shrapnel pieces are used and thrown in the mine field which leads to the collision of these pieces with the other mines and causes explosion. This explosion helps in exploring the maximum explosive mine. The purpose of mine blast algorithm is to find the explosive mine which causes maximum number of causalities. The maximum explosive mine describes the optimal location while number of causalities defines the objective function. Figure 6 shows the schematic view of the mine blast algorithm. Figure 6 illustrate a schematic view of the mine blast algorithm.

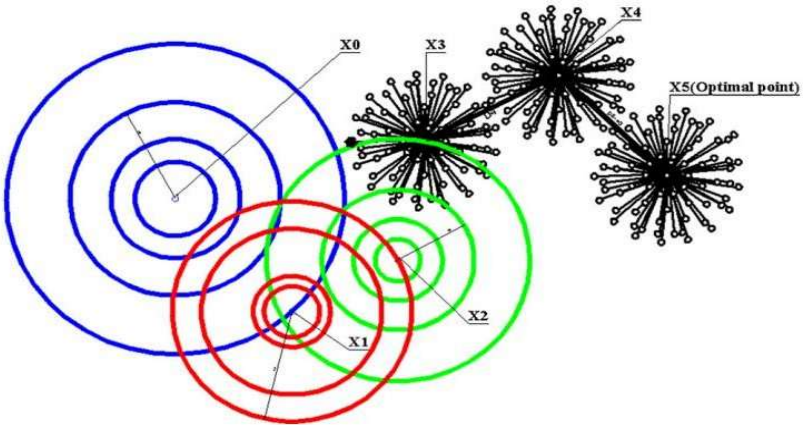

Figure 6. Schematic view of the mine blast algorithm.

In this algorithm, initial point is also named as the shot point, denoted by x_0^f. However, f represents the quantity of shot points. The shrapnel pieces N_s are produced by this shot. These shrapnel pieces acts as individuals inside a population. In order to get an idea of exploding mine Eq 24 is used.

$$X_{n+1}^f = X_{e(n+1)}^f + exp\left(-\sqrt{\frac{m_{n+1}^f}{d_{n+1}^f}}\right) X_n^f \quad \text{n=0,1,2,3……Eq(24)}$$

here, $X_{e(n+1)}^f$ represent mine bomb's location which is the target of the shrapnel,d_{n+1}^f explains the distance between the mine and shrapnel while m_{n+1}^f is the direction (slope) of the thrown shrapnel pieces in every iteration. To calculate the X_{n+1}^f the following equation is used.

$$X_{e(n+1)}^f = d_n^f * rand * \cos(\theta) \quad , \quad \text{…….Eq(25)}$$

ISSN: 3107-6513

In the above equation, the randomly distributed rand is in the range of [0,1] whereas θ represents the angle exhibited by the shrapnel. To calculate the angleθ=360/ N_s is used. In order to improve the value of the blast point the previous information of the solution is considered by using Eq26

$$X_{n+1}^{f} = X_{e(n+1)}^{f} + exp\left(-\sqrt{\frac{m_{n+1}^{f}}{d_{n+1}^{f}}}\right) X_{n}^{f} \quad \text{n=0,1,2,3,} \qquad \text{Eq26}$$

To find the distance d_{n+1}^{f}Eq27 while to calculate the direction of shrapnel pieces Eq 28 is considered.

$$d_{n+1}^{f} = \sqrt{\left(X_{n+1}^{f} - X_{n}^{f}\right)^{2} + \left(F_{n+1}^{f} - F_{n}^{f}\right)^{2}} \quad \text{N= 0, 1, 2,3, ...} \qquad \text{Eq (27)}$$

$$m_{n+1}^{f} = \frac{F_{n+1}^{f} - F_{n}^{f}}{X_{n+1}^{f} - X_{n}^{f}} \quad \text{n= 0,1,2, 3, ...} \qquad \text{Eq (28)}$$

2.5 Grey Wolf Optimizer

This technique has been developed in 2014 [20]. In this algorithm, the natural behaviour of grey wolf is considered in order to evaluate near optimal solution. Grey wolfs exhibits a hierarchy to catch the pray. It uses the leadership hierarchy and the hunting mechanism of grey wolf to find the optimization. The different type of grey wolves α, β, δ and ω are implemented as for hunting, searching prey, encircling prey, and attacking prey. Figure 3 depicts catching pray strategy of grey wolf. Figure 7 depicts the catching pray strategy of Grey wolf.

Figure 7. Catching Pray strategy of Grey wolf

3. GREY WOLF OPTIMIZATION

In the diverse field of engineering, the solution to the optimization problems is a very hot topic of research. From studying the literature, we come to know that over the decades, there are multiple algorithms developed for the finding optimum solution. Mostly, the information of the gradient is required to solve the optimization problem as linear and non-linear programming tools are used by the numeric algorithms.

ISSN: 3107-6513

Optimization algorithms use different methods to find the optimum. It is the most beneficial tool provided by the optimization algorithms. On the other hand, in the field of engineering, there are complex real world optimization problems and finding solution to these problems is a challenging task.

Similarly, to finding the gradient becomes difficult when there are several peaks of the objective function. Due to the computational complexity and the additional disadvantages of the numerical algorithms, the researchers have been focused more to the meta- heuristic algorithms. These algorithms use the natural phenomena to solve problems [21].

3.1 Basic Concept of Grey Wolf Optimization (GWO)

As described earlier, grey wolf algorithm focuses on the natural hunting behavior of the grey wolf for catching the pray. Grey wolfs exhibits a hierarchy to catch the pray. In GWO, the fittest solution considers as the alpha, second, third and the next solutions are described as beta, delta and omega respectively as described in figure 8.

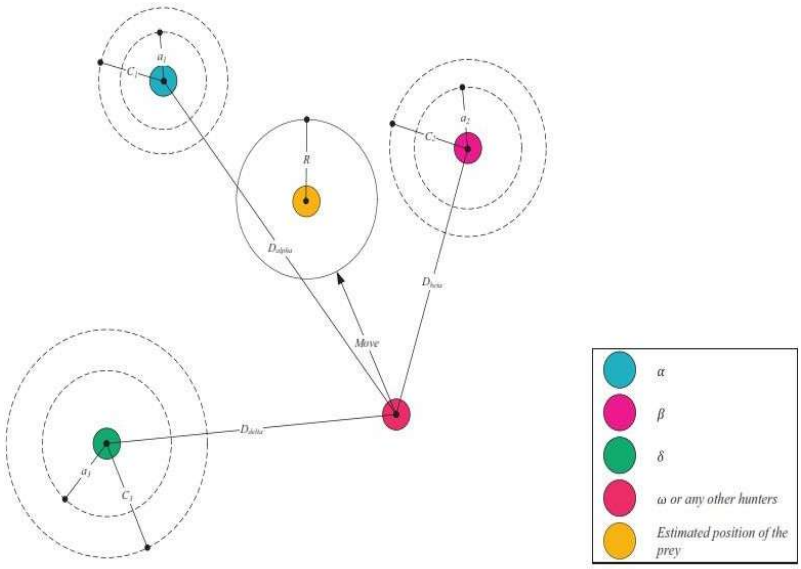

Figure 8. Grey wolf Optimization

3.2 Mathematical Model of GWO

GWO involves three stages to complete the task,i) Encircling prey, ii) Hunting and iii) Attacking

Mathematical model of encircling:

$$\overrightarrow{D} = |\overrightarrow{C} \cdot \overrightarrow{X_P}(t) - \overrightarrow{X}(t) \quad \text{Eq(29)}$$

$$\overrightarrow{X}(t+1) = \overrightarrow{X_P}(t) - \overrightarrow{A} \cdot \overrightarrow{D} \quad \text{Eq (30)}$$

Where t indicates the current iteration $\overrightarrow{A}$ and $\overrightarrow{C}$ are coefficient vectors, $\overrightarrow{X_P}$is position vector ofprey and $\overrightarrow{X}$indicates the position vector of grey wolf. Coefficient vectors can be calculated as:

$$\overrightarrow{A} = 2\overrightarrow{a} \cdot \overrightarrow{r_1} - \overrightarrow{a} \quad \text{Eq(31)}$$

$$\overrightarrow{C} = 2 \cdot \overrightarrow{r_2} \quad \text{Eq(32)}$$

Where $\overrightarrow{r_1}, \overrightarrow{r_2}$ are random vectors and$\overrightarrow{a}$→is linear component which decreases form 2 t 0 with iterations. Grey wolves can recognize the location of prey and encircle them. For the mathematical simulation, alpha is considered as the best candidate solution. It is also assumed that prey's location is known to the beta and delta candidate. Hence these three candidates are considered as the best solution candidate so their value is saved. The location of all other agents is changed accordingly.

The formulas in this regard are as follows:

ISSN: **3107-6513**

$$\overrightarrow{D_\alpha} = \left|\overrightarrow{C_1} \cdot \overrightarrow{X_\alpha} - \overrightarrow{X}\right|, \overrightarrow{D_\beta} = \left|\overrightarrow{C_2} \cdot \overrightarrow{X_\beta} - \overrightarrow{X}\right|, \overrightarrow{D_\delta} = \left|\overrightarrow{C_3} \cdot \overrightarrow{X_\delta} - \overrightarrow{X}\right| \quad \text{Eq(33)}$$

$$\overrightarrow{X_1} = \overrightarrow{X_\alpha} - \overrightarrow{A_1} \cdot \left(\overrightarrow{D_\alpha}\right), \overrightarrow{X_2} = \overrightarrow{X_\beta} - \overrightarrow{A_2} \cdot \left(\overrightarrow{D_\beta}\right), \overrightarrow{X_3} = \overrightarrow{X_\delta} - \overrightarrow{A_3} \cdot \left(\overrightarrow{D_\delta}\right) \quad \text{Eq(34)}$$

$$\overrightarrow{X}(t+1) = \frac{\overrightarrow{X_1} + \overrightarrow{X_2} + \overrightarrow{X_3}}{3} \quad \text{Eq(35)}$$

Where $\overrightarrow{X}(t+1)$the position of grey wolf after first iteration and the final position would be in random place within the circle which is defined by the positions of alpha, beta and delta in search space. These three wolves estimate the position of prey and other wolves change their positions randomly around the prey. Figure 9 describes the flow chart and the pseudo code of grey wolf algorithm.

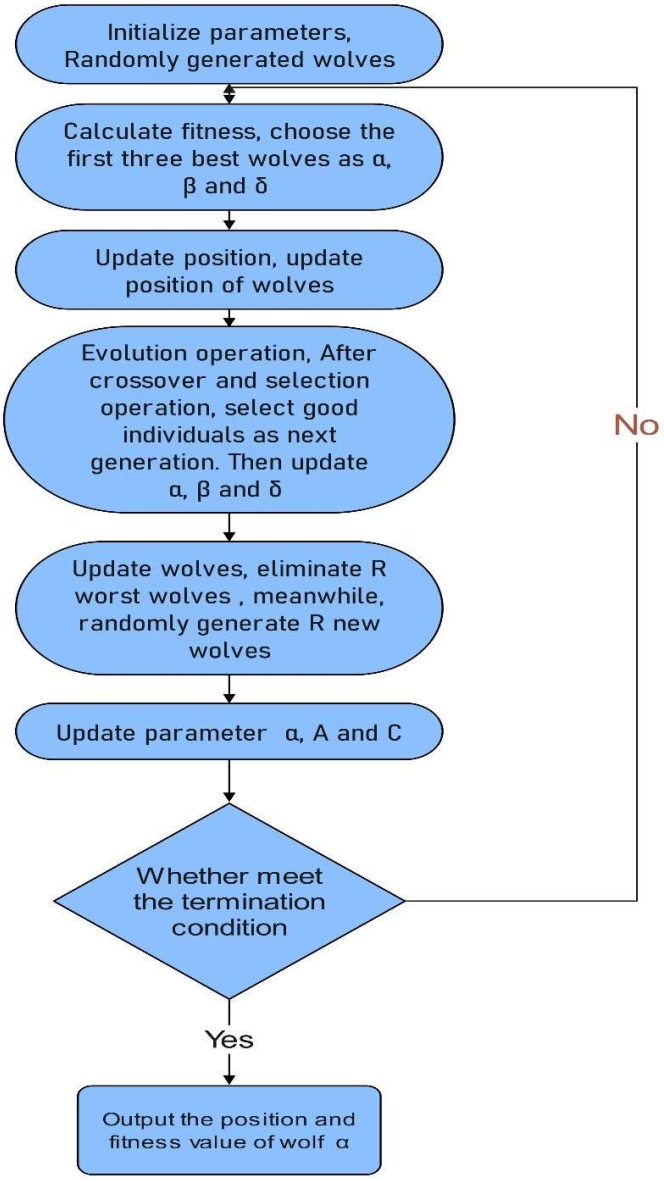

ISSN: 3107-6513

Figure 9. Flow Diagram of Grey Wolf Optimization

Input: Problem Size, *Population* size
Output: Pg _ best
Start
Initialization of the population of grey wolves Xi (i = 1, 2, ... , n)
Initialization of a, A, and C
Calculation of the fitness values of search agents and grading of agents.
(Xα = the best solution in the search agent, Xβ = the second best solution in the search agent, and Xδ = the third best solution in the search agent)
t= 0
While (t < Maximum number of iterations)
For each search agent
Updating the position of the current search agent by Equation
End for
Updating of a, A, and C
Calculation of the fitness values of all search agents and grading them
Updating the positions of Xα, Xβ, and Xδ
t= t+1
End while
End

Figure 10. Pseudo code of Grey Wolf Optimization

3.3 Problem Formulation for Reconfiguration

Although the power losses in a distribution network can occur in a variety of devices that make up the system, the loss produced by power line segment and transformer often take a great share on the entire loss. The power losses produced by the ith line segment connect bus i to bus i + 1 is calculated [52] as:

$$P_{loss}(i, i+1) = R_i . \left(\frac{P_I^2 + Q_I^2}{|V_i^2|}\right) \quad \text{Eq(36)}$$

In which Pi and Qi denote the active and reactive powers emitting from bus i. Considering a network comprised of N line segments, the net power loss P net loss given within the distribution systems can be expressed as the summation of all losses given in the N power lines and the losses given in other components (e.g. transformers, switches, fuses, capacitors):

$$P_{loss}^{net} = \sum_{i=1}^{Nbr} R_i . \left(\frac{P_I^2 + Q_I^2}{|V_i^2|}\right) \quad \text{Eq(37)}$$

Where, N bus represents the entire buses within the systems. Both DNR connection have an effect in the operational attributes of the distribution networks. An indicator of power losses change in the system after applyingDNR denotes the loss reduction index, characterized as the ratio of the power losses of the base systems and the total power losses after DNR interconnection:

$$\Delta P_{loss}^{ratio} = \frac{P_{loss}^{rec}}{P_{loss}^{init}} \quad \text{Eq (38)}$$

ISSN: 3107-6513

where P_{loss}^{rec} and P_{loss}^{init} are the total power loss after DNR and the first net power loss of the systems, respectively. Owing to topology alterations and/or reconfiguration, load of the line segments may differ. Thereupon, the voltages of load bus is changed. The sign of the nonconformity in voltage level is shown below:

$$\Delta V_D = \max_{i=1,\ldots,N_{bus}} \left(\frac{V_1 - V_I}{V_1}\right) \quad \text{Eq (39)}$$

where V1 refers to the voltage level of the source bus and Vi denotes load bus voltage level. After using the standard process of [12], the configuration and DG placement procedure results in the minimization of the sum of the two scalar values conforming to voltage deviations and loss reduction index:

$$\min F = P_{loss}^{ratio} + \Delta V_D \quad \text{Eq (40)}$$

$$V_i^{min} \leq V_i \leq V_i^{max} \quad \text{Eq (41)}$$

Another constrain though out the DNR allocation problems is to uphold the radial configuration of the networks. The size of the search spaces is calculated as C(Ns, Nts), where Ns is the number of switches, Nts is the number of tie lines, and C(n, k) refers to the numbers of k-combination of the n-element sets. Clearly, the number of combinations grows rapidly with both Nbr and Nts.

4. RESULTS AND DISCUSSION

The present part demonstrates the outcomes gotten by Strawberry Plant Propagation Algorithm strategy. The calculation examined in the previous segments is customized and executed on Matlab 2016. Various correlations have likewise been accomplished for demonstrating the legitimacy of the proposed calculation in reducing receptive and genuine system loses and expanding voltage profiles in relationship with different calculations in open writing.

4.1 Results Using IEEE-33 Bus Test System

To lead this examination study and test purposes 33-Bus testing framework is utilized during the exploration, the power current investigation is finished by utilizing the Newton Raphson Method. Below table summarized the results produced by GWO. The comparison shows that network reconfiguration by changing the tie switches from 33–37 to 7, 32, and 34–37 significantly improved system performance. After reconfiguration, active power losses decreased from 208.46 kW to 158.77 kW, achieving a substantial reduction of 23.84%, while reactive power losses were reduced from 111.67 kVAR to 107.31 kVAR, corresponding to a 3.91% improvement. Additionally, the minimum bus voltage increased from 0.91075 pu to 0.92124 pu, indicating enhanced voltage profile and overall system reliability following the reconfiguration. Table 2 represents the simulation results of IEEE 33 Bus Distribution Network.

Table 2: Simulation Results of IEEE 33 Bus Distribution Network

Description	Before Reconfiguration	After Reconfiguration
Tie switches	33 34 35 36 37	7 32 34 35 36 37
Active Power loss (KW)	208.4592	158.7715
Active Power loss Reduction	-	23.8357%
Reactive Power loss (KVAR)	111.6727	107.3094
Reactive Power loss Reduction	-	3.9072%
Minimum voltage (pu)	0.91075	0.92124

ISSN: 3107-6513

This figure illustrates the comparison of bus voltage magnitudes before and after network reconfiguration for the 33-bus system. After reconfiguration using the Grey Wolf Optimization algorithm and updated open switches, the voltage profile shows a noticeable improvement across most buses. The minimum bus voltage is increased, and overall voltage levels are more uniform, indicating enhanced voltage stability and better power quality throughout the distribution network.

The selection of optimal locations is based on the below map represented as an in figure 10 and

Figure 10. Initial and Final Voltages on IEEE-33 Bus Network after reconfiguration

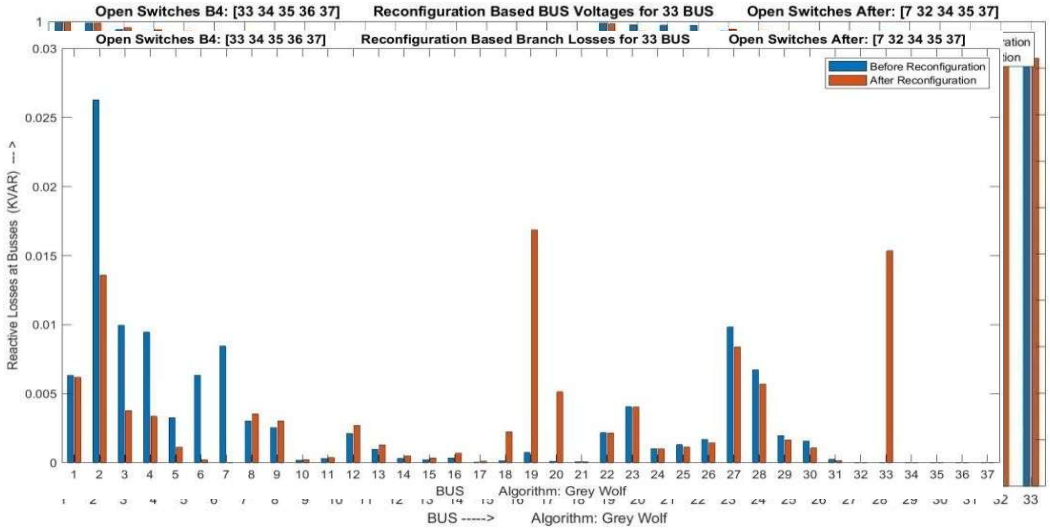

Figure 11. Initial and Final Reactive Power losses for IEEE-33 Bus Network after reconfiguration.

Also figure 12 depicts the Initial and Final Active Power losses on IEEE-33 Bus Network after reconfiguration and figure 13 shows the Convergence Curve of Grey Wolf for IEEE-33 Bus Network after reconfiguration.

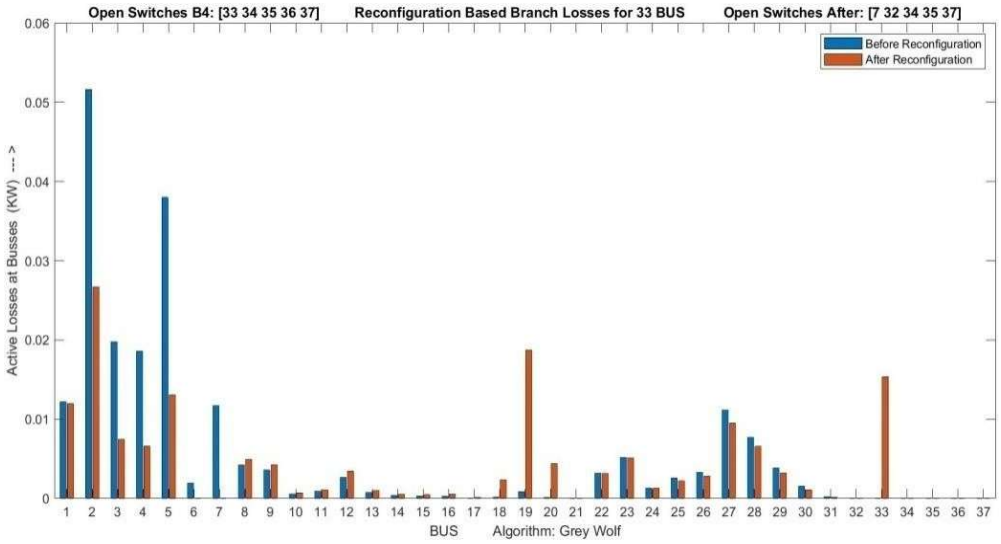

ISSN: **3107-6513**

Figure 12. Initial and Final Active Power losses on IEEE-33 Bus Network after reconfiguration

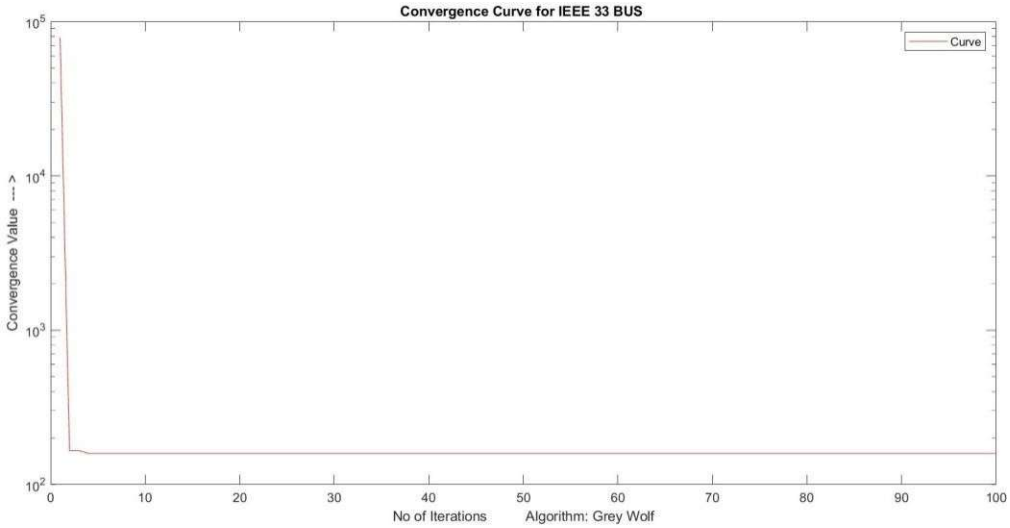

Figure 13. Convergence Curve of Grey Wolf for IEEE-33 Bus Network after reconfiguration

Table 3 illustrate the Active & Reactive Power Demand and Voltage change in IEEE-33 Bus network

Table 3: Active & Reactive Power Demand and Voltage change in IEEE-33 Bus network

Bus	Type	Pd (MW)	Qd (MVAR)	Vm (Before) pu	Vm (After) pu	Percentage Change
1	3	0	0	1	1	**0**
2	1	0.1	0.06	0.997024919	0.997054807	**0.00298882**
3	1	0.09	0.04	0.982947778	0.986985125	**0.403734732**
4	1	0.12	0.08	0.975504447	0.982496938	**0.699249124**
5	1	0.06	0.03	0.968120619	0.978195417	**1.007479782**
6	1	0.06	0.02	0.956103821	0.971685582	**1.558176049**
7	1	0.2	0.1	0.952604971	0.971047112	**1.844214141**
8	1	0.2	0.1	0.939049412	0.95462317	**1.557375844**
9	1	0.06	0.02	0.932763742	0.947805958	**1.504221614**
10	1	0.06	0.02	0.926950079	0.941449131	**1.44990521**
11	1	0.045	0.03	0.926087792	0.940501252	**1.441346008**
12	1	0.06	0.035	0.924584226	0.938832577	**1.424835126**
13	1	0.06	0.035	0.918454812	0.931874079	**1.341926709**
14	1	0.12	0.08	0.916181992	0.929216882	**1.303489056**
15	1	0.06	0.01	0.914765893	0.927435588	**1.266969553**
16	1	0.06	0.02	0.913394302	0.925629748	**1.223544506**
17	1	0.06	0.02	0.91136164	0.922630538	**1.126889832**
18	1	0.09	0.04	0.910752942	0.921575969	**1.08230266**
19	1	0.09	0.04	0.996496487	0.995017683	**-0.147880441**
20	1	0.09	0.04	0.992918434	0.977867539	**-1.50508951**
21	1	0.09	0.04	0.99221384	0.973140207	**-1.907363357**

ISSN: 3107-6513

22	1	0.09	0.04	0.99157634	0.972490192	**-1.908614772**
23	1	0.09	0.05	0.979361654	0.983414017	**0.405236303**
24	1	0.42	0.2	0.972689757	0.976770101	**0.408034411**
25	1	0.42	0.2	0.969364399	0.973458731	**0.409433281**
26	1	0.06	0.025	0.954188132	0.969914184	**1.572605208**
27	1	0.06	0.025	0.951642473	0.967568251	**1.592577848**
28	1	0.06	0.02	0.940283619	0.957094791	**1.681117202**
29	1	0.12	0.07	0.932123576	0.94959675	**1.747317439**
30	1	0.2	0.6	0.928591331	0.946403055	**1.781172357**
31	1	0.15	0.07	0.924459753	0.942996146	**1.8536393**
32	1	0.21	0.1	0.923550844	0.942324669	**1.877382569**
33	**1**	**0.06**	**0.04**	**0.923269218**	**0.921237291**	**-0.20319271**

Table 4 shows the result of the IEEE-33 Active Power Comparison.

Table 4: IEEE-33 Active Power Comparison before and after Reconfiguration

1	**2**	**Before & After Reconfigure Active Loss**		
From Bus	**To Bus**	**Before**	**After**	**Percentage Change**
1	2	12.2025	11.9675	**1.925782548**
2	3	51.6024	26.6782	**48.3004268**
3	4	19.7843	7.48821	**62.15068088**
4	5	18.5835	6.59413	**64.51624933**
5	6	38.0041	13.0677	**65.61503929**
6	7	1.91783	0.06194	**96.77023969**
7	8	11.6983	0	**100**
8	9	4.20217	4.91685	**-17.0076433**
9	10	3.56567	4.24202	**-18.96853575**
10	11	0.55658	0.6754	**-21.34925985**
11	12	0.88572	1.09597	**-23.73755703**
12	13	2.68016	3.4211	**-27.64574004**
13	14	0.73297	0.97398	**-32.8800416**
14	15	0.35885	0.54398	**-51.59268601**
15	16	0.28294	0.4776	**-68.79635463**
16	17	0.25296	0.51215	**-102.4636959**
17	18	0.05342	0.15548	**-191.069805**
2	19	0.16098	2.33575	**-1350.990023**
19	20	0.83229	18.71	**-2148.011437**
20	21	0.10077	4.39318	**-4259.537821**
21	22	0.04364	0.04537	**-3.963729363**
3	23	3.18195	3.15538	**0.835203652**
23	24	5.1442	5.10117	**0.836582437**

ISSN: 3107-6513

24	25	1.28758	1.27678	**0.839423808**
6	26	2.5642	2.21116	**13.76809882**
26	27	3.28192	2.81626	**14.18856144**
27	28	11.1407	9.51061	**14.63184792**
28	29	7.72221	6.56022	**15.04738032**
29	30	3.84033	3.21642	**16.24625256**
30	31	1.57088	1.08466	**30.95224537**
31	32	0.21015	0.11804	**43.82842355**
32	33	0.01298	0	**100**
21	8	0	15.3452	**0**
9	15	0	0	**0**
12	22	0	0	**0**
18	33	0	0.01912	**0**
25	29	0	0	**0**
Total		**208.45917**	**158.7715**	**23.83568478**

Table 5: IEEE-33 Reactive Power Comparison before and after Reconfiguration

1	**2**	**Before & After Reconfigure Reactive Loss**		
From Bus	**To Bus**	**Before**	**After**	**Percentage Change**
1	2	6.313023787	6.191448676	**1.925782548**
2	3	26.28267461	13.5880306	**48.3004268**
3	4	9.94619248	3.764566132	**62.15068088**
4	5	9.464872737	3.358491844	**64.51624933**
5	6	3.24821512	1.116897493	**65.61503929**
6	7	6.339485362	0.204750182	**96.77023969**
7	8	8.442540698	0	**100**
8	9	3.019031339	3.532497421	**-17.0076433**
9	10	2.537107811	3.018360013	**-18.96853575**
10	11	0.184016553	0.223302726	**-21.34925985**
11	12	0.292875046	0.362396427	**-23.73755703**
12	13	2.108705114	2.691672248	**-27.64574004**
13	14	0.964802473	1.282029927	**-32.8800416**
14	15	0.319378125	0.484153878	**-51.59268601**
15	16	0.206625433	0.348776199	**-68.79635463**
16	17	0.33773387	0.683788475	**-102.4636959**
17	18	0.041885819	0.121916971	**-191.069805**
2	19	0.153614297	2.228928129	**-1350.990023**
19	20	0.749957074	16.8591208	**-2148.011437**
20	21	0.117727001	5.132353141	**-4259.537821**
21	22	0.057700906	0.059988013	**-3.963729363**
3	23	2.174194185	2.156035236	**0.835203652**
23	24	4.062086101	4.028103402	**0.836582437**

ISSN: 3107-6513

24	25	1.007506094	0.999048848	**0.839423808**
6	26	1.306099687	1.126274591	**13.76809882**
26	27	1.670984009	1.433895416	**14.18856144**
27	28	9.82254447	8.385324701	**14.63184792**
28	29	6.727407863	5.715109216	**15.04738032**
29	30	1.956108092	1.638313831	**16.24625256**
30	31	1.552500465	1.071966711	**30.95224537**
31	32	0.244936045	0.137584438	**43.82842355**
32	33	0.020182312	0	**100**
21	8	0	15.34515004	**0**
9	15	0	0	**0**
12	22	0	0	**0**
18	33	0	0.019116787	**0**
25	29	0	0	**0**
Total		**111.672715**	**107.3093925**	**3.907241317**

4.2 Results Using IEEE-69 Bus Test System

To lead this examination study and test purposes 33-Bus testing framework is utilized during the exploration, the power current investigation is finished by utilizing the Newton Raphson Method. Informational index of 33-Bus system is given in table 1.

Table 6: Simulation Results of IEEE 69 Bus Distribution Network

Description	Before Reconfiguration	After Reconfiguration
Tie switches	69 70 71 72 73	**15 45 58 63 69**
Active Power loss (KW)	225.0007	**119.271**
Active Power loss Reduction	-	**46.9908%**
Reactive Power loss (KVAR)	102.1648	**96.6971**
Reactive Power loss Reduction	-	**5.3518%**
Minimum voltage (pu)	**0.90919**	**0.94828**

ISSN: **3107-6513**

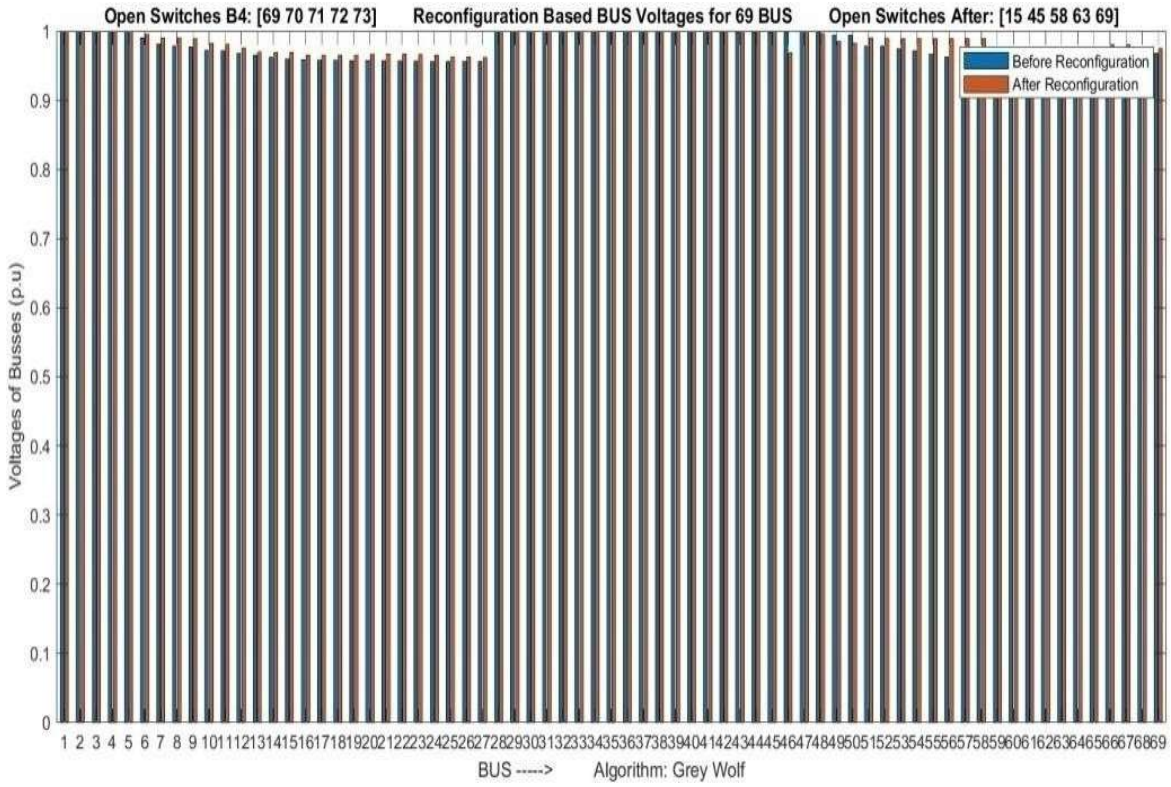

Figure 14. Initial and Final Voltages on IEEE-69 Bus Network after reconfiguration

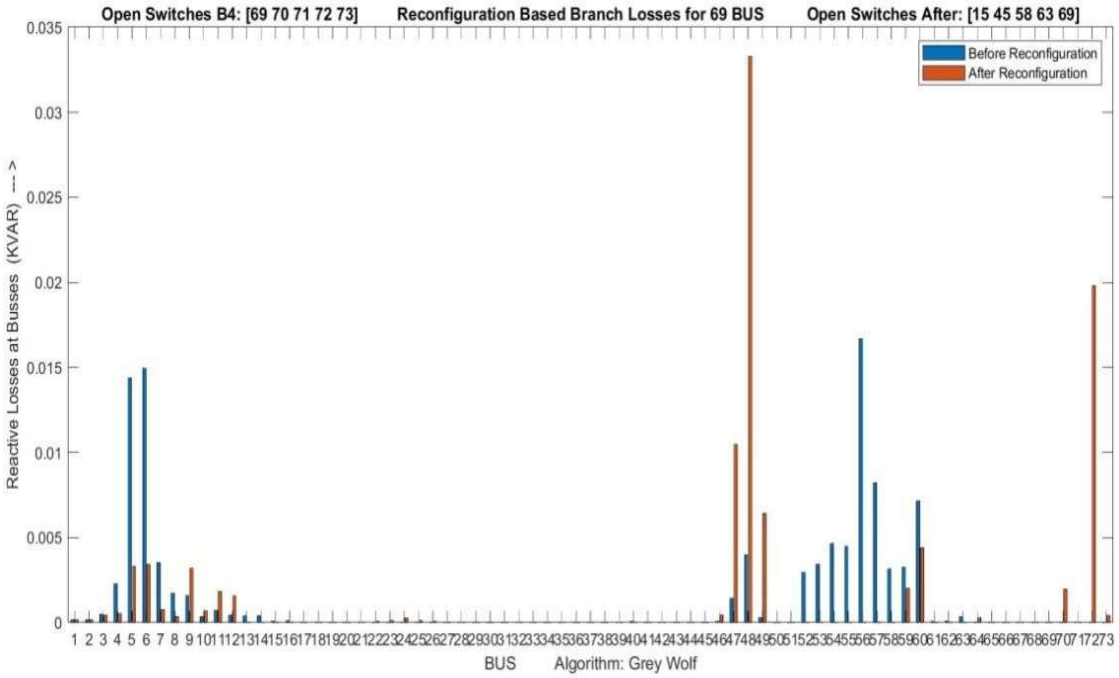

ISSN: **3107-6513**

Figure 15. Initial and Final Reactive Power losses for IEEE-69 Bus Network after reconfiguration

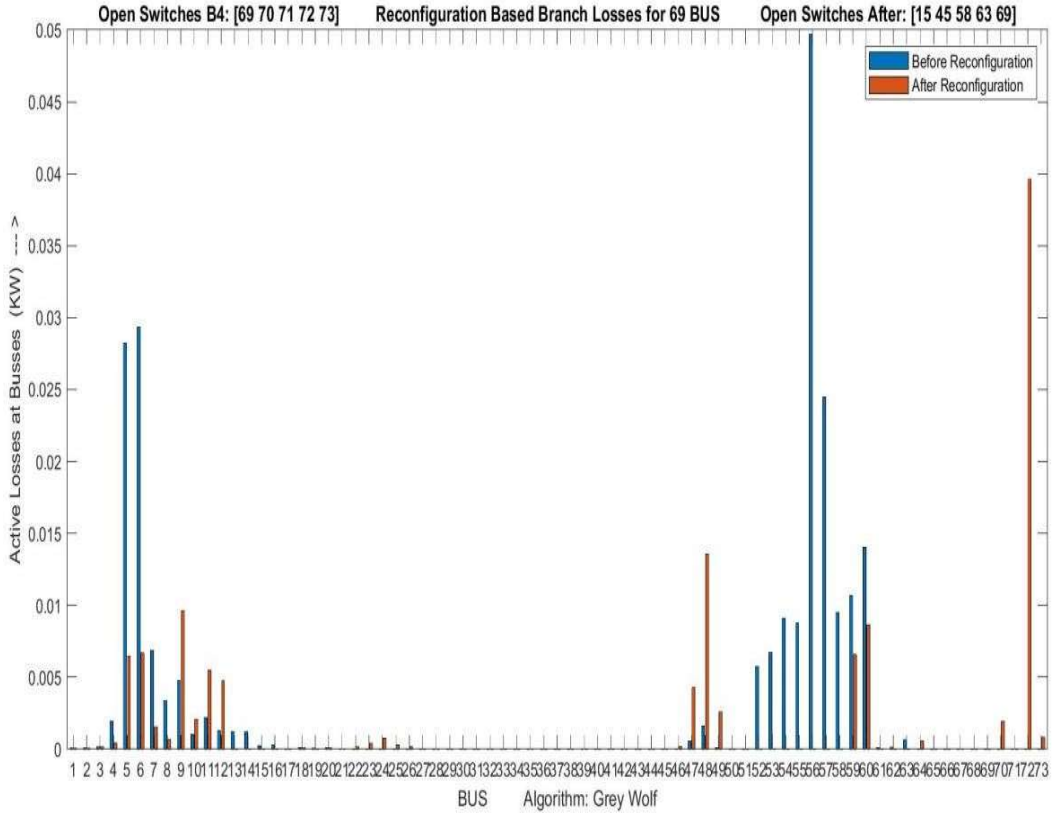

Figure 16. Initial and Final Active Power losses on IEEE-69 Bus Network after reconfiguration

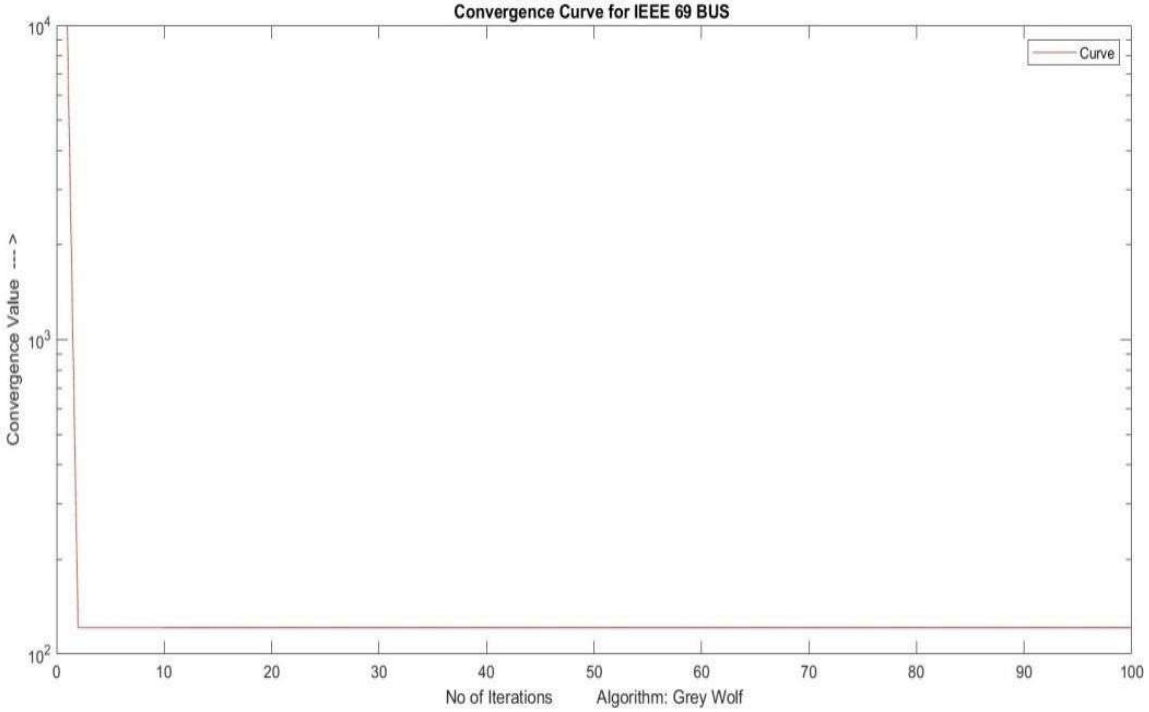

Figure 17. Convergence Curve of Grey Wolf for IEEE-69 Bus Network after reconfiguration

ISSN: 3107-6513

Table 7: IEEE-69 voltage comparison before and after RECONFIGURATION

Bus	Type	Pd (MW)	Qd (MVAR)	Vm (Before) pu	Vm (After) pu	Percentage Change
1	3	0	0	1	1	**0**
2	1	0	0	0.999966496	0.999966732	**2.36014E-05**
3	1	0	0	0.999932992	0.999933464	**4.7201E-05**
4	1	0	0	0.99983945	0.999849413	**0.000996509**
5	1	0	0	0.999020278	0.99965863	**0.063897819**
6	1	0.0026	0.0022	0.990084977	0.997594086	**0.758430757**
7	1	0.0404	0.03	0.98079135	0.995453309	**1.494911135**
8	1	0.075	0.054	0.978575317	0.994967467	**1.675103563**
9	1	0.03	0.022	0.977441847	0.994757971	**1.771575859**
10	1	0.028	0.019	0.972441594	0.992143962	**2.026072118**
11	1	0.145	0.104	0.971340065	0.991586877	**2.084420519**
12	1	0.145	0.104	0.96817849	0.990472706	**2.302696853**
13	1	0.008	0.0055	0.965252734	0.989428047	**2.504557871**
14	1	0.008	0.0055	0.962353516	0.98949268	**2.820082541**
15	1	0	0	0.959483427	0.989623673	**3.141299273**
16	1	0.0455	0.03	0.958950116	0.989106674	**3.144747379**
17	1	0.06	0.035	0.958069518	0.988253022	**3.150450343**
18	1	0.06	0.035	0.958060607	0.988244384	**3.150508118**
19	1	0	0	0.957595536	0.987793559	**3.15352591**
20	1	0.001	0.0006	0.957296591	0.987503771	**3.155467213**
21	1	0.114	0.081	0.956814373	0.987036322	**3.158601113**
22	1	0.0053	0.0035	0.956807469	0.98702963	**3.158646012**
23	1	0	0	0.956735621	0.986959984	**3.159113331**
24	1	0.028	0.02	0.956579236	0.986808391	**3.160130742**
25	**1**	**0**	**0**	**0.956410151**	**0.986644488**	**3.161231284**
26	1	0.014	0.01	0.956340399	0.986576874	3.16168539
27	1	0.014	0.01	0.956320848	0.986557921	3.161812692
28	1	0.026	0.0186	0.999926083	0.999926555	4.72016E-05
29	1	0.026	0.0186	0.999854389	0.999854861	4.72084E-05
30	1	0	0	0.999733264	0.999733737	4.72198E-05
31	1	0	0	0.999711891	0.999712363	4.72219E-05
32	1	0	0	0.999605022	0.999605495	4.7232E-05
33	1	0.014	0.01	0.999348822	0.999349294	4.72562E-05
34	1	0.0195	0.014	0.999013327	0.9990138	4.72879E-05
35	1	0.006	0.004	0.998945915	0.998946387	4.72943E-05
36	1	0.026	0.0186	0.999919182	0.999893528	-0.002565659
37	1	0.026	0.0186	0.99974735	0.999342628	-0.040482403
38	1	0	0	0.999588853	0.998761906	-0.082728701
39	1	0.024	0.017	1	0.998594278	-0.140572164
40	1	0.024	0.017	1	0.99858485	-0.14151499
41	1	0.0012	0.001	1	0.994967815	-0.503218486
42	1	0	0	1	0.993432942	-0.656705814
43	1	0.006	0.0043	1	0.993230174	-0.676982647

ISSN: 3107-6513

44	1	0	0	1	0.99318372	-0.681628008
45	1	0.0392	0.0263	1	0.992633882	-0.736611769
46	1	0.0392	0.0263	1	0.99262964	-0.737036021
47	1	0	0	1	0.999694274	-0.030572617
48	1	0.079	0.0564	1	0.995837292	-0.416270849
49	1	0.3847	0.2745	1	0.98314162	-1.685838015
50	1	0.3847	0.2745	1	0.980103079	-1.989692116
51	1	0.0405	0.0283	1	0.994932607	-0.506739272
52	1	0.0036	0.0027	1	0.994923228	-0.507677189
53	1	0.0043	0.0035	1	0.994676196	-0.532380352
54	1	0.0264	0.019	1	0.99458853	-0.541146956
55	1	0.024	0.0172	1	0.994530126	-0.546987428
56	1	0	0	1	0.994530126	-0.546987428
57	1	0	0	1	0.994530126	-0.546987428
58	1	0	0	1	0.994530126	-0.546987428
59	1	0.1	0.072	1	0.950082599	-4.99174011
60	1	0	0	1	0.945195892	-5.480410774
61	1	1.244	0.888	1	0.938001414	-6.199858643
62	1	0.032	0.023	1	0.937719767	-6.228023291
63	1	0	0	1	0.937342708	-6.265729188
64	1	0.227	0.162	1	0.935494788	-6.450521205
65	1	0.059	0.042	1	0.9349363	-6.50636996
66	1	0.018	0.013	1	0.991531302	-0.846869784
67	1	0.018	0.013	1	0.991530655	-0.846934471
68	1	0.028	0.02	1	0.990150184	-0.984981608
69	1	0.028	0.02	1	0.990149153	-0.985084697

Table 8: IEEE-69 Active power comparison before and after reconfiguration

1	**2**	**Before & After Reconfigure Active Loss**		
From Bus	**To Bus**	**Before**	**After**	**Percentage Change**
1	2	0.017316	0.072633	-319.4577538
2	3	0.004999	0.072633	-1352.925867
3	4	0.000198	0.153657	-77331.11325
4	5	0.048683	0.103984	-113.5933208
5	6	0.020104	1.516263	-7442.243272
6	7	0.002659	1.56566	-58784.58507
7	8	0.000513	0.333065	-64790.96496
8	9	0.006076	0.115904	-1807.710954
9	10	1.26E-05	1.32127	-10526202.42
10	11	0.023285	0.262863	-1028.909501
11	12	0.582813	0.276659	52.53046448
12	13	1.633506	0	100
13	14	0.115897	0.000627	99.45890524
14	15	0.001757	0.002542	-44.66755645
15	16	4.38E-05	0.210626	-480844.3041
16	17	5.781071	0.30153	94.78417826

ISSN: **3107-6513**

17	18	6.711472	0.002451	99.9634779
18	19	9.124758	0.098066	98.925278
19	20	8.790163	0.063042	99.28280838
20	21	49.68488	0.10116	99.79639639
21	22	24.48933	0.000507	99.99793012
22	23	9.505751	0.004829	99.94919945
23	24	10.67107	0.010511	99.9015016
24	25	14.02633	0.005683	99.95948158
25	26	0.112053	0.002344	97.90770082
26	27	0.134933	0.000329	99.75643796
3	28	0.66117	0.000347	99.94753965
28	29	0.041212	0.002583	93.73167003
29	30	0.002624	0.005829	-122.1197959
30	31	1.53E-05	0.001029	-6612.080679
31	32	0.023324	0.005143	77.95063033
32	33	3.71E-05	0.012293	-33066.47706
33	34	0	0.010403	#DIV/0!
34	35	0	0.000479	#DIV/0!
3	36	0	0.011991	#DIV/0!
36	37	0	0.157959	#DIV/0!
37	38	0	0.234139	#DIV/0!
38	39	0.004999	0.067596	-1252.150725
39	40	0.000198	0.003617	-1722.910954
40	41	0.048683	1.315707	-2602.590756
41	42	0.020104	0.556785	-2669.577955
42	43	0.002659	0.073639	-2669.577955
43	44	0.000513	0.01607	-3030.837925
44	45	0.006076	0.190216	-3030.837925
45	46	1.26E-05	0.001302	-10273.39973
4	47	0.023285	0.222284	-854.6390705
47	48	0.582813	5.563763	-854.6390704
48	49	1.633506	17.82304	-991.091141
49	50	0.115897	3.62588	-3028.533325
8	51	0.001757	0.0017	3.268103688
51	52	4.38E-05	4.24E-05	3.268160115
9	53	5.781071	0.005014	99.9132747
53	54	6.711472	0.004931	99.92653568
54	55	9.124758	0.001563	99.98287083
55	56	8.790163	1.26E-26	100
56	57	49.68488	1.89E-26	100
57	58	24.48933	0	100
58	59	9.505751	0	100
59	60	10.67107	10.09453	5.402810989
60	61	14.02633	13.26852	5.402810744
61	62	0.112053	0.105975	5.424793402
62	63	0.134933	0.127609	5.427520954

ISSN: **3107-6513**

63	64	0.66117	0.625285	5.427520955
64	65	0.041212	0.038973	5.432669949
11	66	0.002624	0.002518	4.042483028
66	67	1.53E-05	1.47E-05	4.042485666
12	68	0.023324	0.022285	4.453973817
68	69	3.71E-05	3.54E-05	4.453978426
11	43	0	0	#DIV/0!
13	21	0	0	#DIV/0!
15	46	0	1.175162	#DIV/0!
50	59	0	59.12401	#DIV/0!
27	65	0	0	#DIV/0!
Total		284.4188	121.0991	57.4222607

Table 9: IEEE-69 reactive power comparison before and after reconfiguration

1	**2**	**Before & After Reconfigure Reactive Loss**		
From Bus	**To Bus**	**Before**	**After**	**Percentage Change**
1	2	3.923199094	2.808638451	28.4094846
2	3	3.92312646	2.808464154	28.41260197
3	4	3.283507291	2.373709591	27.70810657
4	5	0.66233377	0.474450172	28.36690604
5	6	0.662229786	0.474328374	28.37405027
6	7	0.658113523	0.471356156	28.37768255
7	8	0.616147863	0.440558742	28.49788686
8	9	0.496713056	0.355388078	28.45203613
9	10	0.411885645	0.293623208	28.71244445
10	11	0.382564375	0.274186495	28.32931844
11	12	0.20129898	0.144098807	28.41553032
12	13	0	0	#DIV/0!
13	14	-0.008	-0.0055	31.25
14	15	-0.016000627	-0.011000207	31.25139935
15	16	0.342601078	0.225364864	34.2194528
16	17	0.296890453	0.195295227	34.21976856
17	18	0.236588923	0.160195522	32.28950853
18	19	0.176586471	0.125194688	29.10289969
19	20	0.176488406	0.125162269	29.08187473
20	21	0.175425363	0.124541434	29.00602755
21	22	0.061324203	0.043508	29.0524816
22	23	0.056023696	0.040007834	28.58765765
23	24	0.056018867	0.040006237	28.58435166
24	25	0.028008356	0.020002762	28.58287842
25	26	0.028002673	0.020000883	28.57509225
26	27	0.014000329	0.010000109	28.57233005

ISSN: **3107-6513**

3	28	0.091538106	0.065218858	28.75223103
28	29	0.065537759	0.046618007	28.86847593
29	30	0.039535175	0.02801169	29.14742546
30	31	0.039529347	0.028009763	29.14185249
31	32	0.039528318	0.028009423	29.14086864
32	33	0.039523175	0.028007723	29.1359486
33	34	0.025510882	0.018003597	29.42777486
34	35	0.006000479	0.004000158	33.33601739
3	36	0.54800843	0.369361408	32.59932011
36	37	0.521996439	0.350731975	32.80950816
37	38	0.49583848	0.331745716	33.09399549
38	39	0.495604341	0.33147222	33.11757128
39	40	0.471536746	0.314393285	33.32581446
40	41	0.447533128	0.297389065	33.54926242
41	42	0.445017422	0.294851876	33.74374545
42	43	0.444460636	0.294201155	33.80715157
43	44	0.438386997	0.289815303	33.89053402
44	45	0.438370928	0.289795041	33.89273264
45	46	0.398980712	0.263255219	34.01805867
4	47	2.621019864	1.898890653	27.55145892
47	48	2.620797579	1.898341465	27.56626914
48	49	2.536233815	1.828322988	27.91189137
49	50	2.133710772	1.510212494	29.22131183
8	51	0.044101742	0.031000881	29.70599547
51	52	0.003600042	0.002700014	25.00048759
9	53	0.054711507	0.03970586	27.42685737
53	54	0.050406494	0.036203307	28.17729487
54	55	0.024001563	0.017200796	28.3346847
55	56	-7.06656E-14	-4.52701E-17	99.93593764
56	57	3.53441E-14	-1.76438E-14	149.9199477
57	58	0	0	#DIV/0!
58	59	0	0	#DIV/0!
59	60	1.586260887	1.125279869	29.06085761
60	61	1.576166355	1.122215697	28.80093568
61	62	0.318897842	0.227457258	28.6739425
62	63	0.286791867	0.204403291	28.7276541
63	64	0.286664258	0.204338343	28.7185838
64	65	0.059038973	0.042019849	28.82693055
11	66	0.036002533	0.026000769	27.78072238
66	67	0.018000015	0.013000004	27.77781244
12	68	0.056022321	0.040007378	28.58671755

ISSN: 3107-6513

68	69	0.028000035	0.020000012	28.57147586
11	43	0	0	#DIV/0!
13	21	0	0	#DIV/0!
15	46	-0.358604247	-0.236365911	34.08725274
50	59	1.745384894	1.226841883	29.70937889
27	65	0	0	#DIV/0!
Total		38.06472465	26.98225023	29.11481566

5. Conclusion

This research focused on optimizing the configuration of power distribution networks using the Grey Wolf Optimization (GWO) algorithm, aiming to minimize active and reactive power losses while improving voltage profiles. The study was applied to IEEE 33-bus and IEEE 69-bus radial distribution systems, where power flow analysis was conducted using the Newton-Raphson method. The reconfiguration was achieved by strategically altering the positions of sectionalized and tie switches without violating the radial topology or operational constraints of the network.

Simulation results demonstrated that the proposed GWO-based approach significantly enhanced system efficiency. For the IEEE 33-bus system, active power loss was reduced by 23.83%, and reactive power loss decreased by 3.90%, whereas for the IEEE 69-bus system, reductions of 46.99% and 5.35% were achieved, respectively. Moreover, an improvement in the minimum voltage profile was observed in both test systems, confirming the effectiveness of GWO in addressing multi-objective optimization problems in power distribution networks.

Compared to conventional and other meta-heuristic algorithms such as Particle Swarm Optimization (PSO), Artificial Bee Colony (ABC), and Fireworks Algorithm (FWA), GWO demonstrated superior convergence characteristics and computational efficiency. Its ability to balance exploration and exploitation in the search process enables rapid identification of optimal switching configurations, leading to reduced power losses and improved voltage stability. This makes GWO a reliable and efficient optimization tool for large-scale, complex electrical distribution systems.

Overall, the Grey Wolf Optimization algorithm provides a robust, adaptive, and scalable solution for real-time distribution network reconfiguration. Its implementation can significantly contribute to improving the operational performance of modern smart grids, enhancing voltage regulation, and minimizing energy losses. Future research can explore hybrid models combining GWO with other intelligent optimization techniques and extend its application to networks integrated with renewable energy sources and distributed generation to further strengthen grid resilience and sustainability.

References:

[1] M. Ahmadi Kamarposhti *et al.*, "Optimizing capacitor bank placement in distribution networks using a multi-objective particle swarm optimization approach for energy efficiency and cost reduction," *Scientific Reports,* vol. 15, no. 1, p. 12332, 2025.

[2] F. D. P. García-López *et al.*, "Cyber-Physical Electrical Power and Energy System Laboratory for Enabling Modern Power Systems," in *2025 IEEE Kiel PowerTech*, 2025: IEEE, pp. 1-8.

[3] F. Zhang, M. Wang, W. Zhang, and H. Wang, "THATSN: Temporal hierarchical aggregation tree structure network for long-term time-series forecasting," *Information Sciences,* vol. 692, p. 121659, 2025.

[4] P. Schavemaker and L. Van der Sluis, *Electrical power system essentials*. John Wiley & Sons, 2025.

[5] M. Bilal and M. Rizwan, "Integration of electric vehicle charging stations and capacitors in distribution systems with vehicle-to-grid facility," *Energy sources, part a: recovery, utilization, and environmental effects,* vol. 47, no. 1, pp. 7700-7729, 2025.

ISSN: **3107-6513**

[6] W. Sjöström, "Influence of Inductance on Conductive Charging Systems for Vehicles: A Study of Cable-Induced Inductance and Its Effects on Charging Infrastructure," ed, 2025.
[7] S. Sharma, *Electric Power Transmission and Distribution*. KHANNA PUBLISHING HOUSE, 2025.
[8] M. Treutlein *et al.*, "Generating peak-aware pseudo-measurements for low-voltage feeders using metadata of distribution system operators," *IET Smart Grid,* vol. 8, no. 1, p. e12210, 2025.
[9] A. F. Othman *et al.*, "Optimal Distribution Network Reconfiguration via the Integration of Distributed Generation Penetration using Meta-Heuristic Technique," *Journal of Advanced Research Design,* vol. 139, no. 1, pp. 101-118, 2026.
[10] J. Wong, C. Tan, N. Rahim, R. H. Tan, and S.-C. Yip, "Communication-less adaptive overcurrent relay coordination for service restoration in distribution systems," *Energy Reports,* vol. 13, pp. 256-263, 2025.
[11] H. Li *et al.*, "Resolving Artifacts and Improving the Detection Limit in Circular Differential Scattering Measurement of Chiral and Achiral Gold Nanorods," *ACS nano,* vol. 19, no. 3, pp. 3635-3644, 2025.
[12] P. Garofalo and A. V. Vonella, "A Multi-Objective Evaluation Tool (MUVT) for Optimizing Inputs in Cropping Systems: A Case Study on Three Herbaceous Crops," *Sustainability (2071-1050),* vol. 17, no. 7, 2025.
[13] G. Lidestam, "Exploring heuristic pricing methods to accelerate branch-and-price for the EVRPTW," ed, 2025.
[14] S. K. Ghosh and D. Das, "Performance Assessment of Swarm Intelligence-Based Metaheuristic Algorithms for Lead Core Rubber Bearing Parameter Optimization in Base-isolated Buildings," *Journal of Vibration Engineering & Technologies,* vol. 13, no. 8, p. 578, 2025.
[15] M. Bakirci, "Performance evaluation of low-power and lightweight object detectors for real-time monitoring in resource-constrained drone systems," *Engineering Applications of Artificial Intelligence,* vol. 159, p. 111775, 2025.
[16] Y. TOYODA, T. SHOHDOHJI, and F. YANO, "An Application of Particle Swarm Optimization to Linear Programming Problems."
[17] A. O. Ibrahim *et al.*, "The Artificial Bee Colony Algorithm: A Comprehensive Survey of Variants, Modifications, Applications, Developments, and Opportunities," *Archives of Computational Methods in Engineering,* pp. 1-35, 2025.
[18] M. Liu, Y. Yuan, A. Xu, T. Deng, and L. Jian, "A learning-based artificial bee colony algorithm for operation optimization in gas pipelines," *Information Sciences,* vol. 690, p. 121593, 2025.
[19] M. Ghasemi *et al.*, "Kirchhoff's law algorithm (KLA): a novel physics-inspired non-parametric metaheuristic algorithm for optimization problems," *Artificial Intelligence Review,* vol. 58, no. 10, pp. 1-60, 2025.
[20] A. Ö. Çiftçioğlu, F. Kazemi, and T. Shafighfard, "Grey wolf optimizer integrated within boosting algorithm: Application in mechanical properties prediction of ultra high-performance concrete including carbon nanotubes," *Applied Materials Today,* vol. 42, p. 102601, 2025.
[21] Y. Lu, X. Yu, Z. Hu, and X. Wang, "Convolutional neural network combined with reinforcement learning-based dual-mode grey wolf optimizer to identify crop diseases and pests," *Swarm and Evolutionary Computation,* vol. 94, p. 101874, 2025.

ISSN: **3107-6513**

Author's Biography:

Muhammad Khurshid Ahmad received his M.Sc. degree in Electrical Engineering from the US–Pakistan Center for Advanced Studies in Energy (USPCAS-E), University of Engineering and Technology (UET), Peshawar, Pakistan. He is currently working as an Operation and Maintenance Engineer at Yanbu Al Sania Desalination Plant, Saudi Arabia. His professional experience includes power system operation, maintenance of electrical equipment, and reliability improvement of industrial power networks. His research interests include power system optimization, distribution network reconfiguration, loss reduction techniques, renewable energy integration, and smart grid technologies.

Corresponding Author:

Muhammad Aslam received his Ph.D. degree in Electrical Power Engineering. He is currently serving as a Lecturer at the US–Pakistan Center for Advanced Studies in Energy (USPCAS-E), University of Engineering and Technology (UET), Peshawar, Pakistan. His research interests include power system analysis, smart grid technologies, renewable energy integration, power system optimization, and energy management systems. He has supervised several research projects in the field of electrical power and actively contributes to academic and research activities in advanced energy systems.

Co-Author:

Abdullah Khan received his B.Sc. degree in Energy Engineering and is currently pursuing his M.Sc. degree in Renewable Energy Engineering at the US–Pakistan Center for Advanced Studies in Energy (USPCAS-E), University of Engineering and Technology (UET), Peshawar, Pakistan. His research interests include renewable energy systems, sustainable power generation, energy management, and integration of renewable resources into modern power systems.

No conflicts of interest:

The authors declare that they have **no conflicts of interest** regarding the publication of this paper.